

AMORPHOUS SILICA GEL AS A SURFACTANT FOR SAPONINS: SUPPORT, SYNTHESIS, AND TEXTURE CHARACTERISTICS

Ulugboyeva G.O.¹, Uzokov J.R.¹,
Mukhammadiyev N.Q.¹,
Mukhammadiyev A.N.¹

EMAIL: javlonphd@gmail.com

Received 30th March 2023,

Accepted 19th April 2023,

Online 28th April 2023

ABSTRACT: Silica sorbent samples were synthesized at different temperatures using saponins as surfactants in an acidic medium. The textural properties of the sorbent samples were studied by adsorbing benzene vapor onto them. The specific surface area of the sorbents at different temperatures was found to be 854,2 m²/g, while the pore volume ranged from 0,32 to 0,90 cm³/g. The average diameter of the pores was found to be in the range of 0,8-32,1 nm.

KEYWORDS: sorbent, sol-gel, saponin, surfactant, specific surface area, pore size, and capillary condensation.

¹Samarkand state university, Uzbekistan.

INTRODUCTION

In the last decade, the synthesis of nanomaterials with different physico-chemical properties has increased rapidly [1-4]. It is possible to obtain organic-inorganic hybrid nanocomposite materials by introducing monomers of different functional groups, polymers, and variable-valence metal oxides into the reaction system during the synthesis of these nanomaterials. Based on molecular modeling and design, smart materials with unique physical and chemical properties can be synthesized [2].

Among nano-objects, micro- and mesoporous materials are particularly important and find application in various fields based on their chemical composition, porosity level, textural characteristics, sorption, and catalytic activity [5]. Specifically, micro- and mesoporous materials are used as heat-protective coatings, in alternative energy production, catalysis, chromatography, production of chemical sensors, drug transport in medicine (nanocontainers), virus binding, enzyme immobilization, addressing

ecological problems, and for construction and electronics [6-8]. The role of porous nanomaterials in these applications is incomparable.

Porous silica nanosorbents exhibit unique physical and chemical properties that distinguish them from traditional types. Their high sorption properties are due to their specific surface area and nanometer-sized pores, which make them effective for a wide range of applications [9-10]. The synthesis of specially synthesized MCM-41 (Mobile Composition of Matter) mesoporous silicon materials and their use as a stationary phase in chromatography have opened up new possibilities. Ozin and co-authors [6] were the first to synthesize ordered mesoporous silica materials belonging to the MCM-41 class under acidic conditions, using a dilute solution of tetraethoxysilane and a cationic surfactant at very low pH values [12-16]. Similarly, Zhao et al. [17] synthesized SBA-X (Santa Barbara Amorphous) mesoporous materials with a pore size of 30 nm using a triblock copolymer of nonionic surfactant P123 (Pluronic acid) in an acidic medium

Mesoporous materials belonging to these two classes have found successful application as a stationary phase in high performance liquid chromatography and ion exchange chromatography [18-22]. Despite the synthesis of various micro- and mesoporous materials, there remain challenges in producing thermally stable and selective sorbents for chromatography, as well as improving their textural properties. Therefore, the present work focuses on the synthesis of nano-sized, thermally stable silicon sorbents.

EXPERIMENTAL SECTION

Sorbent samples were synthesized using the sol-gel process in an acidic environment, at temperatures of 35°C, 55°C, and 85°C. The sol-gel process is highly effective in producing nanoporous materials, and it offers several advantages, including a simple one-step method, cost-effectiveness, environmental safety, and low cost. Additionally, it allows for the introduction of functional monomers, polymers, and oxides of metals with variable valency into the reaction system, and the final product's structure can be controlled.

Silica precursor tetraethoxysilane (TEOS, 98% Jinan Xinggao, China), ethanol (EtOH, 96,4%) as a solvent, and 0,1 M solution of HCl acid as a hydrolysis catalyst were used in the synthesis of SiO₂ sorbent samples at different temperatures. To control the pore size of the obtained sorbents, a surfactant solution of saponin in alcohol was used.

RESULTS AND DISCUSSION

The textural properties of the sorbent samples were studied by benzene vapor adsorption using a Mac-Ben-Bakra sensitive quartz spiral setup. The benzene obtained as adsorbate was first purified under vacuum, its vapor pressure was cooled to the vapor pressure given in the table for pure benzene, and the dissolved gases were removed. Before measuring the adsorption of benzene vapor on adsorbents, each adsorption system was vacuumed until the residual pressure was $1,33 \cdot 10^{-3}$ Pa, heated at 298 K for 6 hours, and then adsorption isotherms were obtained (Fig. 1).

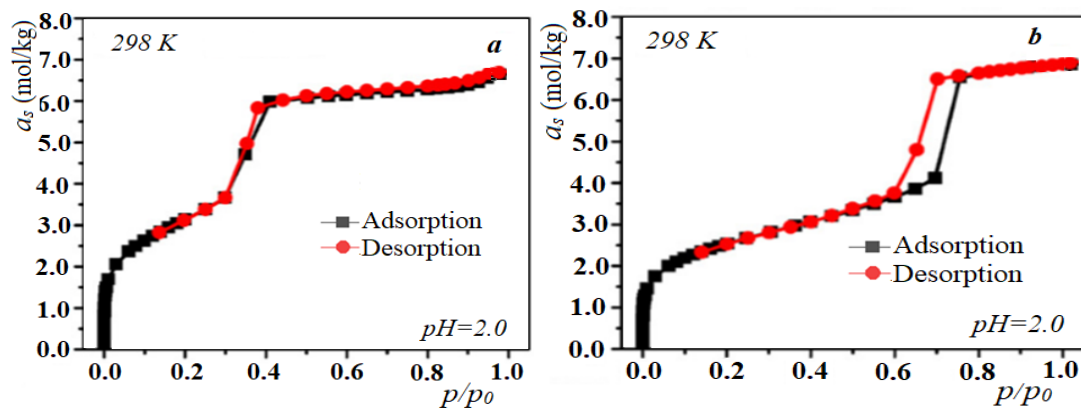


Figure 1 Shows the benzene vapor adsorption isotherms on synthesized sorbents at two different temperatures, namely 35°C (panel *a*) and 55°C (panel *b*).

The results show that the sorbent sample synthesized at 35°C had a higher adsorption capacity for benzene vapor compared to the sorbent synthesized at 50°C. Specifically, the sorption isotherm for the sample synthesized at 35°C exhibited a sharp increase in sorbed benzene from zero relative pressure to $p/p_0=0.1$, followed by saturation at $p/p_0=0.6$, and remained constant thereafter (as shown in Fig. 1*a*). This isotherm is classified as type I according to the IUPAC classification, and it was determined that 85-90% of the total pore volume consisted of micropores.

For the sorbent sample synthesized at 55°C, the adsorption of benzene vapor showed a sharp increase up to the relative pressure of $p/p_0=0.2$, and then approached saturation at $p/p_0=0.8$ (as shown in Fig. 1*b*). The adsorption and desorption lines formed a hysteresis loop at $p/p_0=0.6\div0.8$, which is attributed to the capillary condensation of adsorbed benzene vapor. Based on these observations, it can be inferred that the sorbent sample synthesized at 55°C mainly consists of mesopores, and its adsorption isotherm belongs to type IV H2 according to the IUPAC classification.

The sorption isotherms obtained from benzene vapor adsorption on sorbents synthesized at 85°C revealed the presence of larger mesopores (as shown in Fig. 2*a*). For the sample synthesized at 85°C, hysteresis loops were observed at relative pressures of $p/p_0=0.5\div0.8$, where the adsorption and desorption lines merged. The size of the hysteresis loops increased as the loops shifted towards high relative pressure due to capillary condensation from the adsorption of benzene vapor.

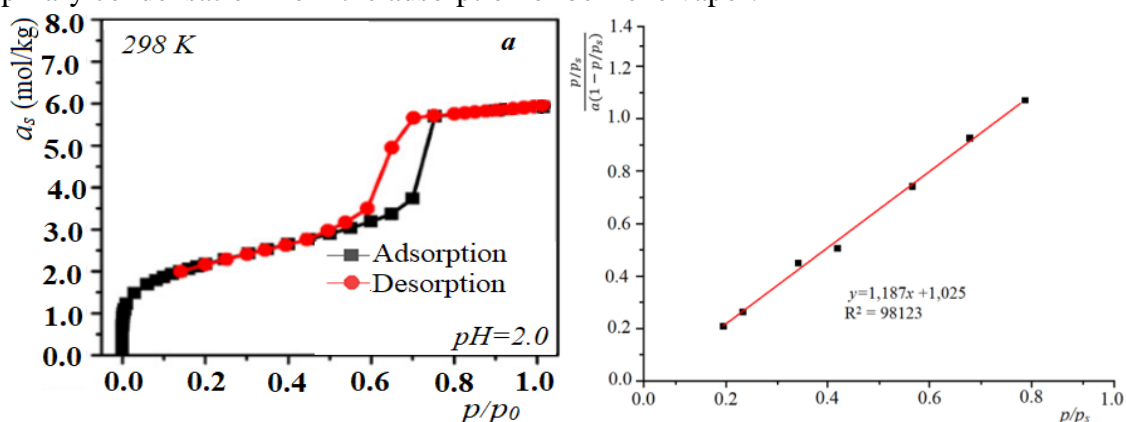


Figure 2 shows the adsorption of benzene vapor on sorbents synthesized at 85°C. Panel (a) displays the sorption isotherms, which reveal the presence of larger mesopores. Panel (b) shows the fit of the sorption data to the BET linear equation

To determine the relative surface area of the sorbents, the following formula was used:

$$S_m = a_m \cdot N_A \cdot \omega_m$$

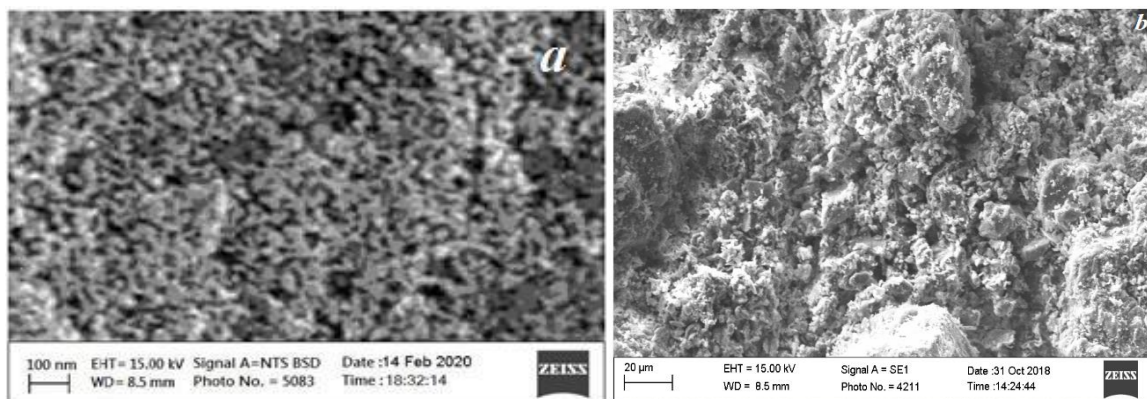
The specific surface area of the sorbent is expressed in square meters per gram ($\text{m}^2 \cdot \text{g}^{-1}$). The monolayer capacity, which is the maximum amount of adsorbate that can be adsorbed onto the sorbent surface, is expressed in moles per kilogram (mol/kg). The Avogadro constant is a physical constant representing the number of constituent particles (such as atoms or molecules) in one mole of a substance. The space occupied by one adsorbate molecule in the saturated monolayer is expressed in square nanometers (nm^2); for example, the value for benzene molecules in silica sorbents is approximately 0,49 nm^2 [10]. Table 1 presents the values of the specific surface area (S_{BET}), pore size (V_s), average diameter (D), monolayer capacity of the adsorbents, and saturation adsorption of the sorbent samples obtained at various temperatures. It is evident from the table that.

Fusion temperature, °C	a_m , mol/kg	S_{BET} , m^2/g	a_s , mol/kg	D , nm
35	1,4±0,2	854,2±18	6,2±0,8	1,2±0,8
55	1,3±0,1	614,9±10	4,5±0,5	6,5±1,02
85	1,3±0,6	600,4±15	3,6±0,2	32,4±5,02

Table 2 presents the results of calculating adsorption volumes using Dubinin's theory of volumetric filling of micropores at a relative pressure of 0,4. The volume of micropores (W_0), mesopores ($W_{\text{mes}} = V_s - W_0$), and saturation adsorption volumes were also calculated.

Fusion temperature, °C	$W_0 \cdot 10^3$, m^3/kg	$W_{\text{me}} \cdot 10^3$, m^3/kg	$V_s \cdot 10^3$, m^3/kg
35	0,32±0,04	0,72±0,02	0,6±0,03
55	0,54±0,01	0,86±0,05	0,28±0,01
85	0,58±0,05	0,96±0,03	0,46±0,08

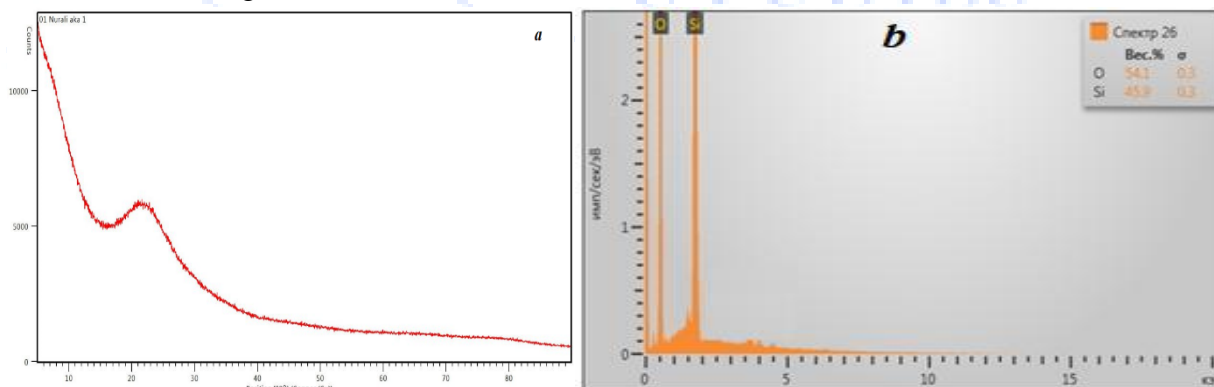
The surface morphology and pore size of the synthesized sorbents were analyzed using a scanning electron microscope (SEM EVO MA 10, Carl Zeiss) equipped with an energy dispersive X-ray spectrometer (EDS Aztec Energy Advanced X-Act, Oxford Instruments). The voltage was increased to 1 kV, and images were taken using a reflection detector (SE2) and back electron beam (ESB) at a magnification of x 200,000 (Fig. 3).



From the pictures, we can see that the sorbent samples synthesized at 55°C consist of ordered spherical components of the same size, and the pores are uniformly distributed throughout the sorbent. In contrast, the sorbents synthesized at 85°C have unevenly distributed pores of different sizes.

The phase composition and structure of the sorbents were analyzed using a Pananalytical Empyran X-ray diffractometer (XRD). To obtain the diffractograms, CuK α -radiation (β -filter, Cu, 1,5406 Å° current mode and tube voltage 30 mA and 30 kV, respectively) and a detector were used at a constant speed of rotation of 4 degrees/min with a step of 0,02° (overlap $\omega/2\theta$), and the scanning angle was varied from 0° to 90°. A rotating camera was used to record the experiments, and its rotation speed was 30 rpm (Figure 4a).

The phase composition of the samples was analyzed using a semi-quantitative method based on calibration standards. The elemental composition of the sorbents was studied using the X-ray microanalysis method (as shown in Figures 4-b).



Based on the XRD analysis, it is possible to see that all the phases present in the sorbents are amorphous. This indicates the high sorption capacity of the sorbents. Moreover, EDS analysis of the sorbents revealed that their elemental composition corresponds to the quantitative ratios of the initial reagents.

CONCLUSIONS

The textural characteristics of sorbent samples synthesized via sol-gel technology at different temperatures were investigated through benzene vapor sorption. The sorbent obtained at 35°C exhibited a specific surface area of $854,2 \pm 18$ m²/g, and 75% of its total pore volume comprised micropores with an average pore diameter of 1,2 nm. In contrast, the sorbents synthesized at 55°C mainly consisted of

mesopores with a specific surface area of $614.9 \pm 10 \text{ m}^2/\text{g}$, and their average pore diameter was found to be four times larger than the sorbents obtained at 85°C .

REFERENCES:

- [1]. Jeevanandam J. Review on nanoparticles and nanostructured materials: history, sources, toxicity and regulations // *Beilstein journal of nanotechnology*. – 2018. – V. 9. – №. 1. – P. 1050-1074.
- [2]. Uzokov J. R., Mukhamadiev N. K. Sorption characteristics of mesoporous composite $\text{SiO}_2 \cdot \text{TiO}_2$ // *Central Asian Journal of Medical and Natural Science*. – 2021. – V. 2. – №. 5. – P. 494-498.
- [3]. Fanizza E. NIR-Absorbing Mesoporous Silica-Coated Copper Sulphide Nanostructures for Light-to-Thermal Energy Conversion // *Nanomaterials*. – 2022. – V. 12. – №. 15. – P. 2545.
- [4]. Gao T., Gao J., Sailor M. J. Tuning the response and stability of thin film mesoporous silicon vapor sensors by surface modification // *Langmuir*. – 2002. – V. 18. – №. 25. – P. 9953-9957.
- [5]. Elma M. Long-Term Performance and Stability of Interlayer-Free Mesoporous Silica Membranes for Wetland Saline Water Pervaporation. *Polymers* 2022, 14, 895. – 2022.
- [6]. Lv H. Characterization and synthesis of new adsorbents with some natural waste materials for the purification of aqueous solutions // *Journal of Environmental Management*. – 2023. – V. 336. – P. 117660.
- [7]. Uzokov J. R., Mukhamadiev N. K. Sorption characteristics of the mesoporous sorbents based on tetraethoxysilane and titanium oxide // *European Journal of Molecular & Clinical Medicine*. – 2020. – V. 7. – №. 07. – P. 656-660.
- [8]. Diyarov A. A. Mukhamadiev N. Q., Uzokov J. R. Synthesis of mesoporous sorbents on the basis of Al_2O_3 and their textural characteristics // *Central Asian Journal of Medical and Natural Science*. – 2022. – V. 3. – №. 3. – P. 511-518.
- [9]. Saleh Medina L. M. et al. High removal of chlorinated solvents by reusable polydimethylsiloxane based absorbents // *Polymer Engineering & Science*. – 2023. – V. 63. – №. 2. – P. 366-378.
- [10]. Arzimurodova X. Ismatov D. M., Uzokov J. R., Mukhamadiyev A. N., Mukhamadiev N. Q. Quantum chemical evaluation of complex formation of Co(II) ions with quercetin molecule // *Central Asian Journal of Medical and Natural Science*. – 2022. – V. 3. – №. 3. – P. 338-344.
- [11]. Usmonova H. Uzokov J. R., Mukhamadiev N. Q., Mukhamadiev A. N. Study of structural and electronic properties of $(\text{ZnO})_n$ ($n = 10 \div 30$) nanoclusters using quantum chemical methods // *Central Asian Journal of Medical and Natural Science*. – 2022. – V. 3. – №. 6. – P. 428-434.
- [12]. Sayitkulov Sh. M. Uzokov, Zh., Saidov, Kh. M., Mukhamadiev, N. K. Study of the texture characteristics of silicon oxide as a catalyst carrier // *XXXV All-Russian Symposium of Young Scientists on Chemical Kinetics*. – 2018. – P. 124-124 (in Russian).
- [13]. Tan J. Z. Y. 3D direct ink printed materials for chemical conversion and environmental remediation applications: a review // *Journal of Materials Chemistry A*. – 2023.
- [14]. Elma M. et al. Hydrogel derived from water hyacinth and pectin from banana peel as a membrane layer // *Materials Today: Proceedings*. – 2023.
- [15]. Tselishchev Yu. G., Kondrashova N. B., Lebedeva I. I. Formation of textural and structural properties of mesoporous silicon oxide // *The Fifth International Conference of the CIS countries "Sol-gel synthesis and study of inorganic compounds, hybrid functional materials and disperse*

- systems" - "Sol-gel 2018". - 2018. - S. 295-295.
- [16]. Chircov C. Mesoporous silica platforms with potential applications in release and adsorption of active agents // *Molecules*. – 2020. – V. 25. – № 17. – P. 3814.
- [17]. Sayari A., Han B. H., Yang Y. Simple synthesis route to monodispersed SBA-15 silica rods // *Journal of the American Chemical Society*. – 2004. – V. 126. – № 44. – P. 14348-14349.
- [18]. Schubert U. Chemistry and fundamentals of the sol-gel process // *The Sol-Gel Handbook*. – 2015. – P. 1-28.
- [19]. Schuth F. Endo-and exotemplating to create high-surface-area inorganic materials // *Angewandte Chemie International Edition*. – 2003. – V. 42. – № 31. – P. 3604-3622.
- [20]. Serban B. A., Barrett-Catton E., Serban M. A. Tetraethyl orthosilicate-based hydrogels for drug delivery effects of their nanoparticulate structure on release properties // *Gels*. – 2020. – V. 6. – № 4. – P. 38.
- [21]. Shahbazi M. A., Herranz B., Santos H. A. Nanostructured porous Si-based nanoparticles for targeted drug delivery // *Biomatter*. – 2012. – V. 2. – № 4. – P. 296-312.
- [22]. Silva R. F., Vasconcelos W. L. Influence of processing variables on the pore structure of silica gels obtained with tetraethylorthosilicate // *Materials Research*. – 1999. – V. 2. – P. 197-200.

